# INJECTION SYSTEM ASSESSMENT TO OPTIMIZE PERFORMANCE AND EMISSIONS OF A NON-ROAD HEAVY DUTY DIESEL ENGINE: EXPERIMENTS AND CFD MODELLING

#### Maddalena Auriemma, Stefano Iannuzzi

Istituto Motori, National Research Council of Italy Viale G. Marconi, 4, 80125 Naples, Italy tel.: +39 081 7177135, +39 081 7177103 e-mail: m.auriemma@im.cnr.it, s.iannuzzi@im.cnr.it

#### Simone Serra

Faculty of Engineering, University of Cagliari Via Università 40, 09124 Cagliari e-mail: s.serra@im.cnr.it

#### Gerardo Valentino

Istituto Motori, National Research Council of Italy Viale G. Marconi, 4, 80125 Naples, Italy tel.: +39 081 7177129 e-mail: g.valentino@im.cnr.it

#### Abstract

The advancing emissions requirements and the customer demand for increased performance and fuel efficiency are forcing the diesel engine technology to keep improving. In particular, the large diesel engines are undergoing to a significant restriction in emission standards. Reaching the new limits requires innovative solutions, improved calibration and controls of the engine combustion technology, as well as the optimization of the injection system that has experienced the most fundamental development over the last decade.

The objective of the paper is to present preliminary results of an investigation for the development of an efficient combustion system for marine diesel engines. The effect of different engine parameters on performance and engine out emissions were evaluated. Specifically, different nozzle geometries, injection pressure, injection timings were taken into account. The investigation was carried out both experimentally and numerically. Three different nozzles geometries for three different values of the start of injection were tested. The in-cylinder pressure, rate of heat release, NOx and soot were evaluated for a high load engine condition.

The experimental activity was carried out on a large displacement single cylinder direct injection diesel engine equipped with a high-pressure common rail injection system able to manage multiple injections. The engine test bench was equipped with an external air supercharger able to set high air boost levels. The system controls the intake air temperature by means of a heater exchanger. The numerical investigation was carried out using the commercial CFD STAR-CD code in a three-dimensional domain including the cylinder head and piston bowl. Combustion behaviour was simulated using the 3 Zones Extended Coherent Flame Model (ECFM3Z).

Keywords: Diesel combustion, heavy duty engines, STAR-CD

## 1. Introduction

The increasing attention for environmental protection has led governments to impose strict reductions on exhaust emissions from internal combustion engines. Diesel off-road and marine engines are undergoing to significant emissions restrictions too. EPA (United States Environmental

Protection Agency) is adopting new standards for emissions of nitrogen oxides (NOx), hydrocarbons (HC), carbon monoxide (CO) and particulate matter (PM) from new diesel-cycle engines with a gross power output at or above 37 kW used in marine vessels. The new standards for marine diesel engines will reduce their emissions of HC by 8 percent, NOx by 15 percent and PM by 11 percent in 2020 [1]. Reaching these limits requires the adoption of a technology that has been mainly developed for and used on land-based engines. In particular, diesel engines employed for non-road and marine applications are characterized by unit displacements higher than 2 dm<sup>3</sup>. These engines, only recently, have been equipped with the common rail injection system and electro-injectors able to manage high pressures (160-200 MPa) and multiple injections. The introduction of turbo chargers, supplied by exhaust gases, with post-refrigerated air allowed achieving a great technological improvement in terms of performance and emissions. The main challenge for these high performance heavy-duty diesel engines is the improvement of gaseous emissions and soot in order to achieve low environmental impact. It is well known, for diesel engines, the NOx-soot trade-off and the severe trouble to break it without reducing the efficiency of the engine. For heavy-duty engines, direct water injection (DWI) has been widely studied being a promising tool to reduce NOx without any important effect on soot [2, 4]. On the other side, water addition has a negative effect on HC emissions, both for the gas phase and as particulate sold organic fraction [3, 4].

An alternative way to control engine emissions and accomplish the request to achieve a sustainable energy economy is the use of biodiesel fuels as alternatives to conventional petroleum-based fuels. Biodiesel has the potential of reducing emissions such as CO, CO<sub>2</sub>, HC and PAH [3, 5, 6] but has a negative impact on NOx production related to its O<sub>2</sub> content (about 10-15 wt. %). This trend has been confirmed by a review published by EPA (Environmental Protection Agency) and Lapuerta et al. that have reported emission data for heavy duty engines fuelled with biodiesel. As heavy duty diesel engines have been mainly designed for maximum fuel efficiency and performance without main concerns of the impact on nitrogen oxides, nowadays these engines have to reduce NOx emissions. In general, the current technology is using advanced controls for charge air temperature and pressure, which are already considered to be emission controllers for light duty engines. However, NOx reductions are to be achieved even through fuel injection control strategies such as rate shaping or EGR optimization.

In the last years, research has also been focused on innovative combustion regimes being available electro-injectors that allow an accurate control of the delivered fuel amount and provide the management of multiple injections [7, 8]. In fact, the last generation of common rail injection systems, characterized by high injection pressure (which leads to a better atomization of jets), allows to control the ignition process and combustion propagation, reducing, in this way, the pressure gradient and peak. Moreover, they allow improving engine specific power without a significant increase in mechanical stress (minor impact on engine life cycle) leading to advantages on the weight/power ratio. Despite important results in terms of engine out emissions have been achieved, further improvements are to be made in order to fulfil future emissions standards. To reach the target of low emissions and high efficiency, innovative combustion mechanisms need to be explored. A promising strategy is a high air-fuel premixing joint to moderate levels of EGR that may enhance the transition from heterogeneous combustion, representative of conventional diesel engines, to a partially homogeneous one [7, 9].

The present investigation is part of an extensive research project focused on the exploration of innovative combustion modes by selecting suitable injection strategies and fuel properties in order to reduce emissions in heavy-duty diesel engines. The results that will be described in this paper are relative to the assessment of different injector nozzles and the calibration of the STAR-CD combustion model. The investigation is carried out for three nozzles and different injection pressures focusing on the combustion behaviour and engine out emissions.

## 2. Engine Apparatus and Test Conditions

Tests were performed on a single cylinder direct injection, 4-stroke heavy-duty marine diesel engine. The engine, 4200 cm<sup>3</sup> displacement, is able to supply 150 kW@1800 rpm rated power at 0.4 MPa boost pressure. The engine is equipped with a common rail injection system and a solenoid electro-injector for multiple injection strategies. The injection system is able to manage pressures up to 160 MPa. The main engine specifications are listed in Tab. 1 while the investigated nozzles characteristics are listed in Tab. 2.

| Engine Type                     |        |  |
|---------------------------------|--------|--|
| Displacement [cm <sup>3</sup> ] | 4200   |  |
| Bore [mm]                       | 170    |  |
| Stroke [mm]                     | 185    |  |
| Connection rod [mm]             | 315    |  |
| Compression ratio               | 13.8:1 |  |
| Power [kW]                      | 150    |  |
| Maximum torque [Nm]             | 796    |  |
| Maximum speed [rpm]             | 2100   |  |

Tab. 1. Engine Specifications

Tab. 2. Nozzle grid and specifications

| Nozzle                          | Hydraulic Flow* | Hole Diameter | Hole Number | Angle |
|---------------------------------|-----------------|---------------|-------------|-------|
| 1                               | 2300            | 0.30 mm       | 8           | 147°  |
| 2                               | 2300            | 0.30 mm       | 8           | 150°  |
| 3                               | 2300            | 0.30 mm       | 8           | 154°  |
| * CM <sup>3</sup> /30 SEC@100MP | A               |               |             |       |

The engine is connected to an asynchronous motor by a HBM T10FS torque sensor, through which the engine torque is acquired. An external oil free supercharging system is able to set intake air pressures up to 0.4MPa using a pressure regulation valve that fine-tunes the flow in order to reach the required value. In addition, the mass flow rate (Kg/h) supplied to the engine is continuously acquired through a flow sensor meter. The in-cylinder pressure signal is measured by a piezo-quartz transducer with an accuracy of  $\pm 0.1\%$  full scale, while the accuracy of analog input signals to the acquisition system (AVL INDICOM 621) is  $\pm 0.01\%$ . Tab. 3 reports the accuracy of the main acquired quantities. NOx emissions are measured by the ABB Limas 11UV analyzer, which operates through the photometric technology being able to measure NOx quantities down to few ppm. Smoke emissions are sampled by the AVL 415S smoke meter (0.1% value resolution) and reported in filter smoke number (FSN).

*Tab. 3. Accuracy of the acquired quantities* 

| Accuracy of measurements  |         |  |
|---------------------------|---------|--|
| Engine Speed              | ±1 rpm  |  |
| Torque                    | ±0.1 Nm |  |
| Mass Flow Rate            | ± 1mg   |  |
| Specific fuel consumption | ±1.5%   |  |
| NOx                       | 5 ppm   |  |
| Smoke                     | ±0.1%   |  |

Tab. 4. Operating Conditions

| Speed [rpm]                   | 1700       |
|-------------------------------|------------|
| P <sub>boost</sub> [MPa]      | 0.31       |
| Torque [Nm]                   | 522        |
| Pinj [MPa]                    | 120 to 160 |
| Injector nozzle angle [deg]   | 147-150-54 |
| Start of Injection [cad BTDC] | 10 – 16    |

## 3. Operating conditions

Engine testes were carried out exploring the effect of different nozzles geometries on combustion behaviour, fuel consumption, and engine out emissions. Tests were performed at the engine speed of 1700rpm setting a boost pressure of 0.31MPa and changing the injection pressure from 120 to 160 MPa with a single injection strategy. The amount of injected fuel was adjusted in order to keep a constant torque of 522Nm at the different investigated starts of injection (10-16 cad BTDC). A summary of the explored parameters are reported Tab. 4. It is important to point out that, in the present paper, the SOI designates the start of the energizing current to the solenoid injector. In fact, there is a delay between the timing of the energizing current to the solenoid and the actual start of fuel discharge from the injector nozzles; this delay, which is due to hydraulic and electronic reasons, was estimated in 0.3 ms (≅3 cad at 1700 rpm) from the instantaneous fuel flow rate profile.

## 4. CFD simulation procedure and mesh generation

The simulation was conducted using the STAR-CD code in a three-dimensional calculation grid, which has the capability to solve the transient, compressible turbulent-reacting flows with sprays on the finite volume grids with moving boundaries and meshes. Piston motion was carried out by cell activation and deactivation supported by vertex motion routines supplied by ES-ICE module. Combustion regimes with n-dodecane fuel were simulated using the ECFM3Z model (3-Zones Extended Coherent Flame Model). The computational domain includes the cylinder head and piston bowl, as shown in Fig. 1. The mesh resolution was set to achieve a good agreement between the simulation and experimental results for the penetration of non-reacting and reacting fuel jets. The number of cells varies from 97571 at TDC and over 191117 at BDC. The mesh generation was done by means of the trimming method because of the good accuracy provided, in terms of stability and computing time. The sequence of the STAR-CD process is briefly described and sketched below in Fig. 2.

The k-ɛ Turbulence Model was used for the predictions of turbulent flow and turbulent viscosity correction while the numerical approximation and computation was based on the pressure-correction method and the PISO algorithm with the second order upwind difference scheme (MARS). The spatial discretization was employed for the continuity, momentum, energy, and turbulence equations. The fuel and air interaction was modelled with the Lagrangian approach. This modelling is an essential component of the process because it strongly affects the atomization and break-up phenomena determining number, dimension, and velocity of droplets. STAR-CD includes several atomization, break-up, and impingement models; in this paper Huh for atomization, Reitz and Diwakar for break-up and Bai for spray impingement models were used.

The fuel was injected with spray characteristics adjusted according to those assumed in the experiments. Because the characteristics of fuel were not completely stated but they strongly influence the simulation, the real fuel was approximated by using the n-dodecane ( $C_{12}H_{26}$ ) virtual

fuel with well-known characteristics, already implemented in the STAR-CD code. The injection rate was computed from the real instantaneous fuel flow delivered from the injector and rectified according to the n-dodecane density.

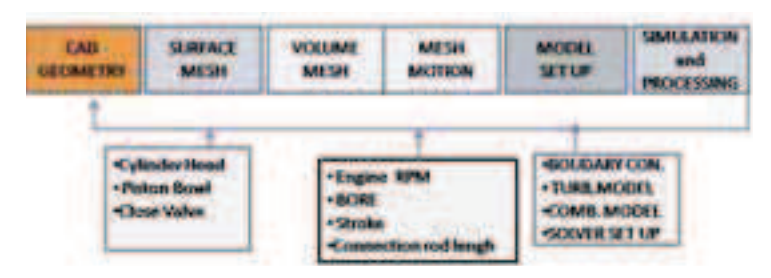


Fig. 1. STAR-CD procedure

The ECFM3Z combustion model, which describes the areas of gas carried out/burnt based on superficial density equation of flames and a mixing model, was used (reference). The combustion model that deals with inhomogeneous turbulent premixed and diffusion combustion is coupled to improved burned gas chemistry, allowing the calculation of CO, soot, and NOx formation. Computation starts at the intake valve closure IVC=127 cad BTDC and ends at 180 cad ATDC, with the initial conditions based on previous CFD simulations of the intake and exhaust fluid-dynamics ducts and experimental data. The constant temperature boundary conditions were allocated independently for the cylinder head, the cylinder wall, and the piston crown that outlines the walls of the combustion chamber.

Simulations were performed at 1700rpm for the selected nozzle geometries and two starts of injection (16 and 10 cad BTDC). To calibrate the combustion process, the motored in-cylinder pressure trace and the computed one were previously compared.

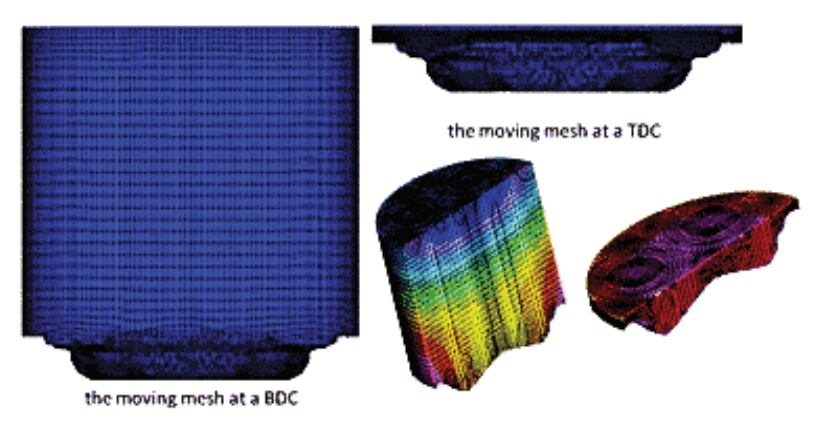


Fig. 2. Moving Mesh Sketch

## 5. Results and Discussion

The first section of this paragraph reports the experimental results of combustion behaviour and engine out emissions for the different explored parameters, such as injector nozzles, injection pressures, and starts of injection. The second section illustrates the results of a CFD computation with the comparison of the main calculated quantities to the experimental data.

#### 5.1. Experiments

The investigation concerned the assessment of the three nozzle spray angles (147°-150°-154°) at fixed engine speed, intake air boost and engine load. In the following paragraphs, the effect of

injection pressure and start of injection on combustion behaviour, engine performance, and engine out emissions will be illustrated.

## 5.1.1. Effect of Injection Pressure on Combustion Behaviour

In this section, the results of injection pressure sweep on combustion behaviour are explained. Tests were performed at the constant speed of 1700 rpm and different injection pressures (120 to 160 MPa), exploring two SOIs (10 and 16 cad BTDC). Fig. 3 reports in-cylinder pressures and rates of heat release for the 150° spray angle nozzle. Because similar trends were obtained for the other two nozzles, the plots are not reported in the discussion.

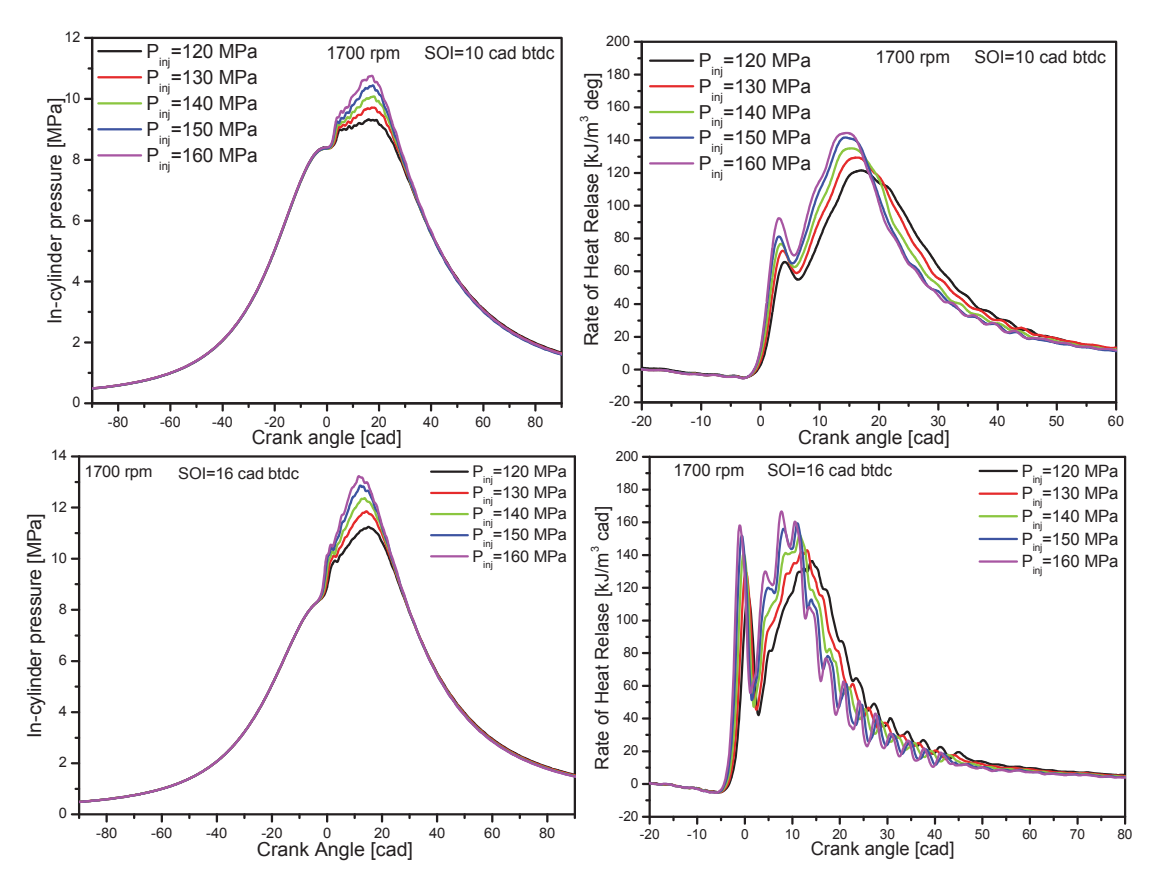


Fig. 3. Combustion pressure and rate of heat release at SOI=10 cad BTDC (top plot) and SOI=16 cad BTDC (bottom plot) for the 150° spray angle nozzle.

Plots highlight that an increase in the injection pressure produces higher peaks for the incylinder combustion pressure both at SOI=10 and 16 cad BTDC. The reason is related to an enhanced fuel atomization and air-fuel mixture formation that lead to a decrease in ignition delay, earlier start of combustion (SOC), a shorter injection interval and combustion period. The shorter injection interval joined to a higher injection pressure also raises the premixed and diffusive combustion peaks in the rate of heat release traces. In fact, the increase in injection pressure typically determines a higher homogeneity of the charge (because of the enhanced air-fuel mixture) and, as consequence, a reduction in soot. On the other side, the increase of flame temperature worsens NOx emissions, determining, for conventional diesel combustion, the well-known NOx-soot trade-off.

In Fig. 4, the trends of ignition delay and thermal efficiency for the three nozzles and two SOIs, as function of injection pressure, are reported. It is possible clearly notice the strong influence of injection pressure and start of injection on ID. The 150° spray angle nozzle shows the highest ignition delay values while the 154° nozzle shows the lowest ones. A possible explanation of this behaviour may be

searched in the different mixing rate and air utilization within the combustion chamber given by the different nozzle angles. Results of Fig. 2 also highlight a uniform decrease of the ignition delay at retarded start of injection (SOI=10 cad BTDC), along the injection pressure sweep.

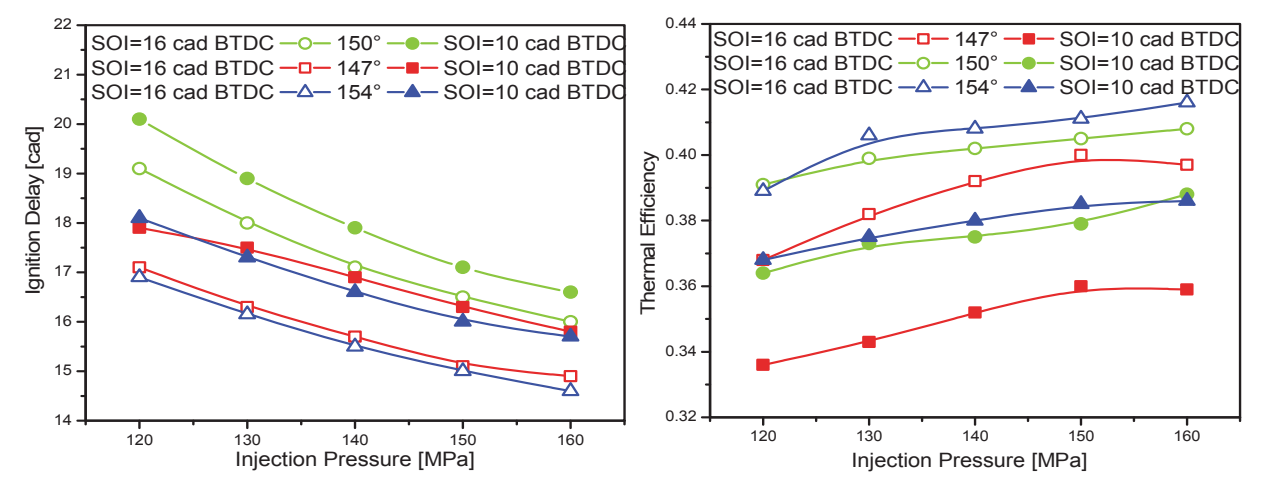


Fig. 4. Ignition delay and thermal efficiency as function of injection pressure

## 5.1.2. Effect of Start of Injection on Combustion Behaviour

In this section, the effect of start of injection on combustion behaviour is described. Fig. 5 reports, for the 150° nozzle, the comparison of the in-cylinder pressure and rate of heat release for the tested starts of injection. From the analysis of the plots, it is possible to observe that a retarded start of injection leads to a lower combustion pressure peak due to the retarded start of combustion (confirmed by the rate of heat release) that brings about lower combustion efficiency.

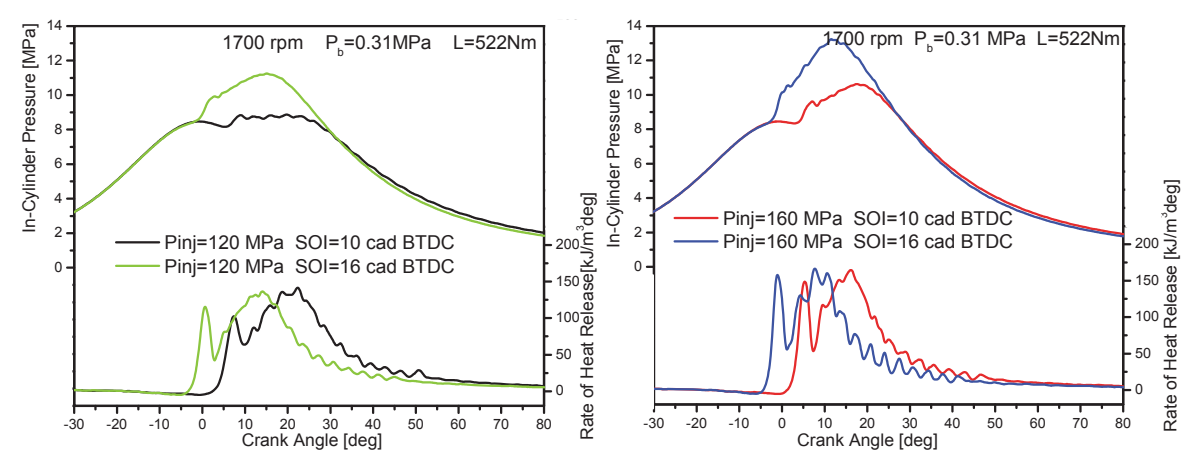


Fig. 5. In-cylinder pressure (left plot) and Rate of Heat Release (right plot) at different SOIs for the 150° nozzle

## 5.1.3. Effect of Injection Pressure and Start of Injection on Engine out Emissions

Figure 6 reports the results of the brake specific fuel consumption and NOx-smoke trade-off as function of injection pressure. The left plot illustrates the behaviour of BSFC for the three investigated nozzles, SOI=10 and 16 cad BTDC in the range of injection pressures between 120 and 160 MPa. The 147° nozzle shows unacceptable values of BSFC particularly at the retarded start of injection (SOI=10 cad BTDC). Moreover, the plot highlights that an increase in the injection pressure and earlier starts of injection (16 cad BTDC vs. 10 cad BTDC) allow a strong reduction in brake specific fuel consumption because of a higher combustion efficiency. The right plot confirms, as expected, that an increase in injection pressure leads to a strong reduction in

smoke but an increase in NOx emissions, reproducing the conventional diesel combustion NOx-Soot trade-off. Comparing the behaviour of the three nozzles, the 150° one shows the best results in terms of engine out emissions and brake specific fuel consumption.

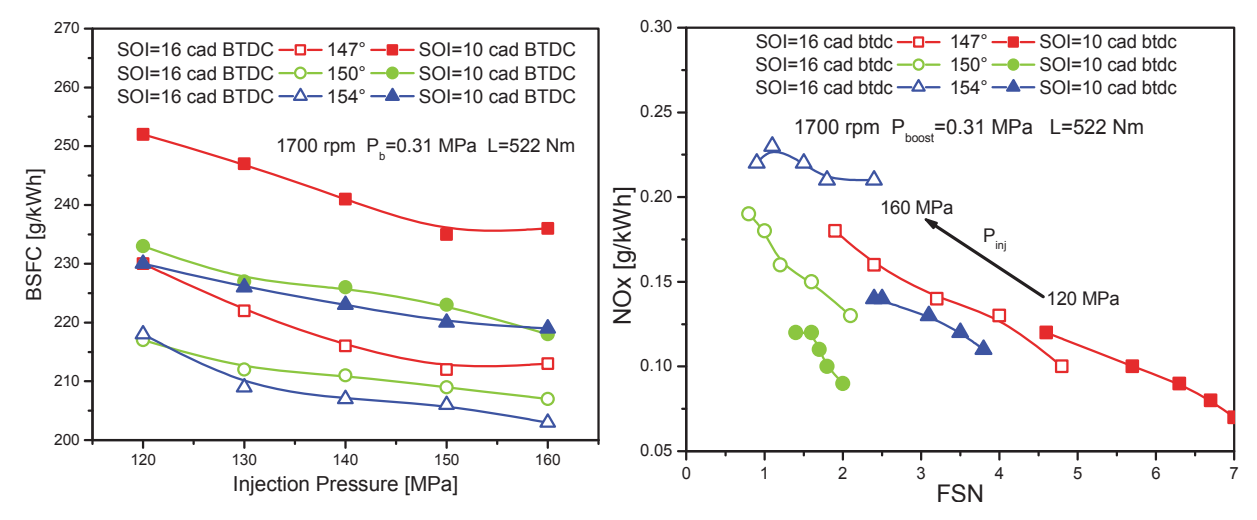


Fig. 6. Brake specific fuel consumption vs. Injection pressure (left plot) and NOx vs. FSN (right plot) for the three investigated nozzles

#### 5.2. CFD results

As well known, performance and emissions of large diesel engines are affected by many parameters that determine the level of air-fuel mixture, combustion efficiency and heat transfer. An analysis of the impact of nozzle geometry on the combustion behaviour was carried out with the STAR-CD code in order to calibrate the combustion model and provide reasonable interpretation of the different nozzles performance. A comparison between simulated and measured in-cylinder pressure trace and rate of heat release was performed to guarantee the prediction reliability. Fig. 7 reports the in-cylinder pressure and rate of heat release traces comparison between the code outputs and experiments, for the three tested nozzles. Plots are relative to the 1700 rpm and SOI=10 cad BTDC engine operative condition. Results show a good agreement between CFD and experiments for the in-cylinder pressure, confirming the validity of the calculation methodology. In addition, a good quality agreement of the premixed combustion peak and the diffusive rate of heat release were captured by the adopted spray and combustion modelling approach. Although the combustion model acceptably detects the start of combustion, it underestimates the premixed peak, probably due to a fast fuel evaporation rate and the computation approach for the heat release calculation. It is useful to remind that the CFD rate of heat release was directly extracted from the reactive species and their respective heat of formation and normalized, while the experimental one was calculated from the in-cylinder pressure according to the well-known thermodynamic model [10].

Considering the experimental results shown in Fig. 6, it is evident that the 147 and 150° nozzles show the worst and the best achievement in terms of NOx-smoke trade-off and fuel consumption. To understand the reasons of this extreme different behaviour, the air-fuel mixing and the evaporation process were explored. The computation was run for the 10 cad BTDC injection timing, analyzing the air-fuel mixing within the combustion chamber, the in-cylinder pressure and rate of heat release.

Figure 8 reports the air-fuel mixing distribution, within the combustion chamber at 20 cad ATDC for the two nozzles (results from the 147° nozzle are shown on the left side). It is well marked the difference in the injected fuel distribution that, for the 150° nozzle reaches a better homogeneity and an enhanced air utilization. The greater homogeneity achieved with the 150° nozzle generates a higher combustion efficiency, as it can be observed from the in-cylinder

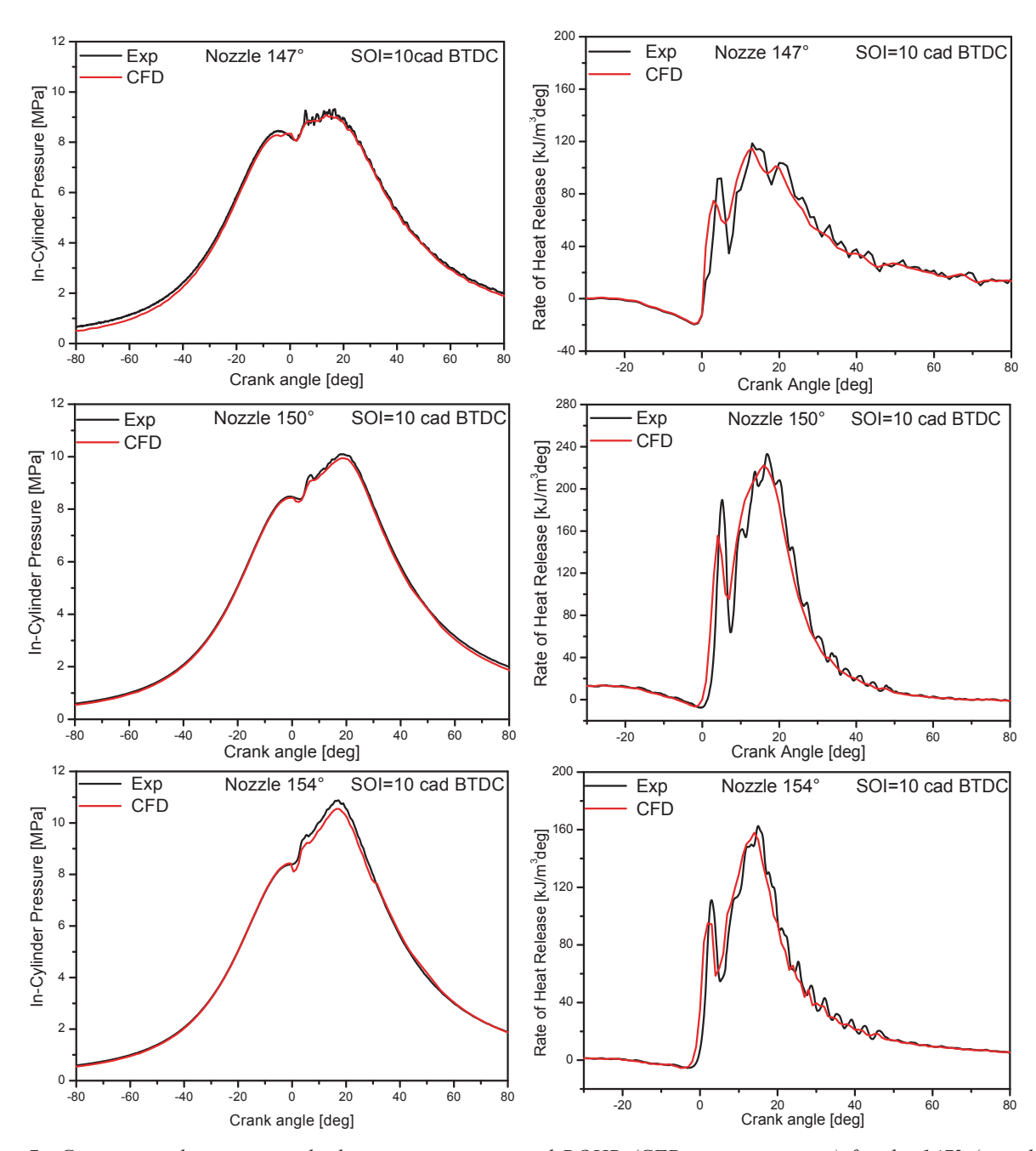


Fig. 7. Comparison between in-cylinder pressure traces and ROHR (CFD vs. experiments) for the 147° (top plot), 150° (middle plot), and 154° (bottom plot) nozzles. (Operative condition: SOI=10 cad BTDC)

pressure and the rate of heat release traces, Fig. 9. In fact, plots show higher peaks in the combustion pressure and for the premixed and diffusive combustion.

In Fig. 10, the injected, evaporated, and burnt fuel is shown for both nozzles. Plots point out that, for the 147° nozzle, about 30 cad after the start of injection the 95% of injected fuel is evaporated, while the same evaporation rate occurs 25 cad after SOI for the 150° nozzle.



Fig. 8. Air-fuel mixing comparison between the 147°(left side) and 150° (right side) nozzles. (Operative condition: SOI=20 cad ATDC)

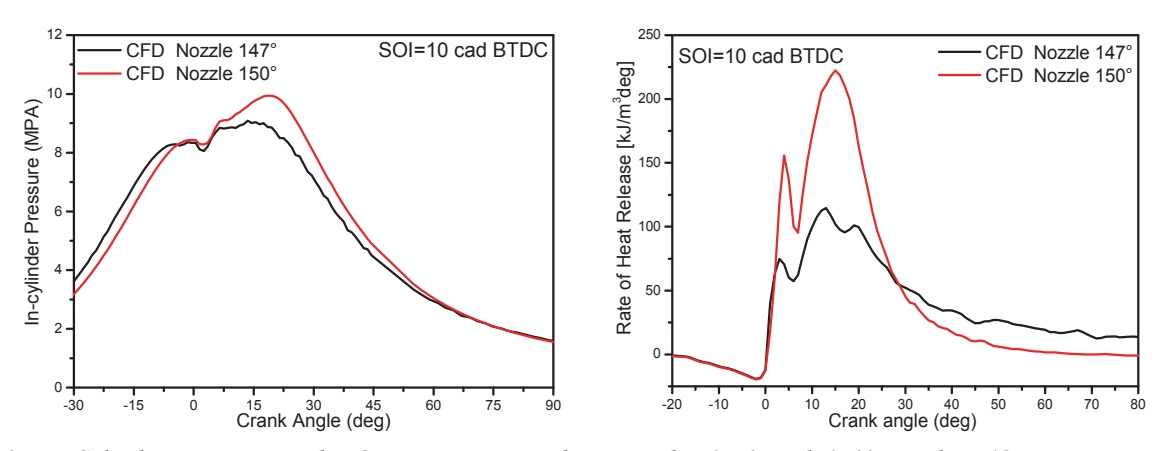


Fig. 9. In-Cylinder pressure and ROHR comparison between the 147° and 150° nozzles. (Operative condition: SOI=10 cad BTDC)

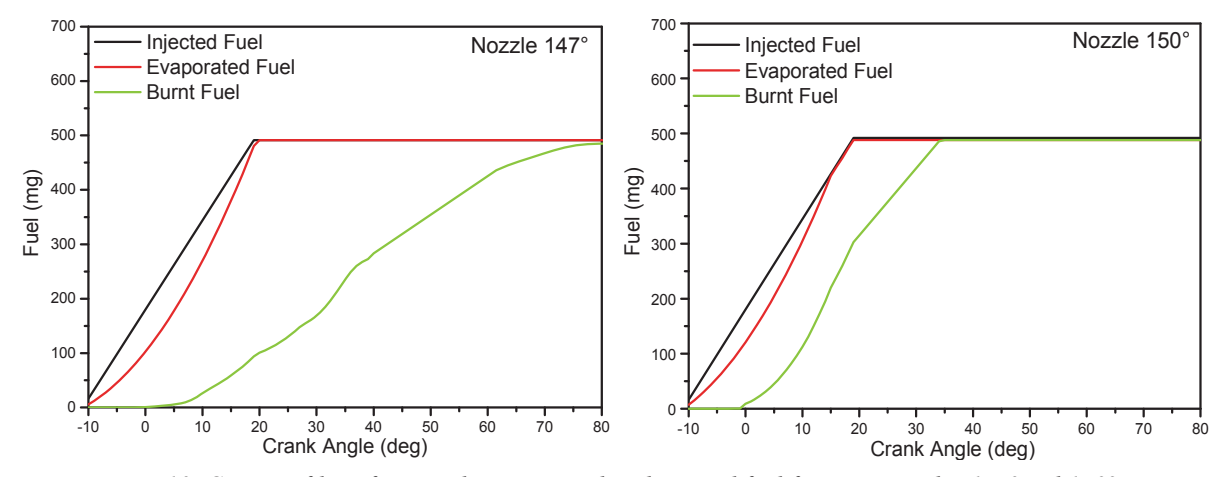


Fig. 10. CFD profiles of Injected, Evaporated and Burned fuel for spray angles 147° and 150°

Further, the 150° nozzle exhibits a shorter combustion interval, which produces a raise in the combustion temperature, as shown in the left plot of Fig. 11. The right plot (same figure) reports the comparison of NOx emissions between experiments and CFD output for the two nozzles. The higher combustion temperature and the higher peak of the rate of heat release, exhibited by the 150° nozzle, produce higher levels of NOx compared to the 147° nozzle. The computed NOx emissions reproduce the experimental trend, but give values about twice higher than those experimentally measured give. As conclusion, it may be pointed out that a wider spray angle (150°) produces a better mixing with a higher combustion efficiency but a worsening in NOx emissions.

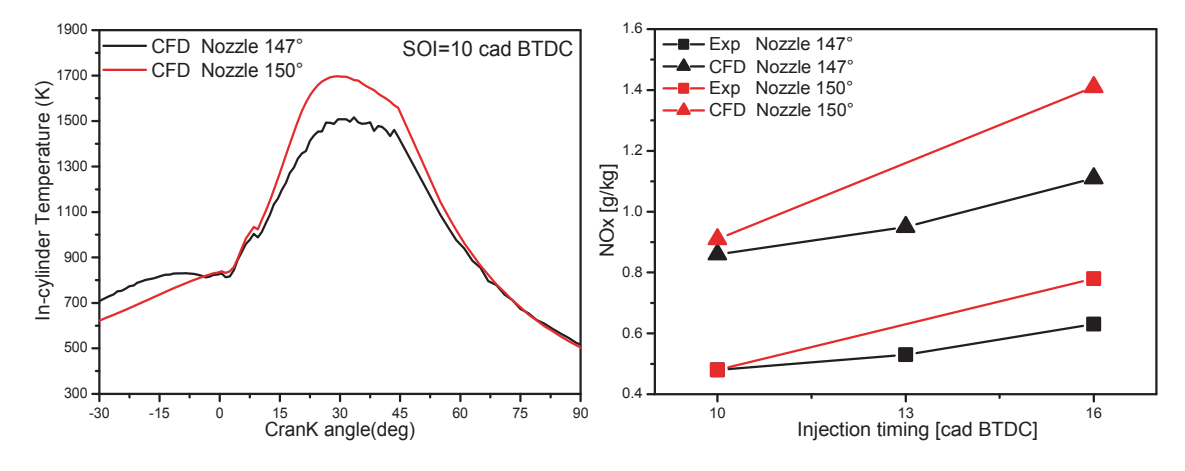


Fig. 11. Temperature (left plot) and NOx (right plot) comparison between the  $147^{\circ}$  and  $150^{\circ}$  nozzles. (Operative condition: SOI = 10 cad BTDC)

#### 6. Conclusions

The paper has illustrated preliminary results of an investigation having the objective of developing an efficient combustion system for marine diesel engines. The investigation was carried out both experimentally and numerically evaluating the effect of different engine parameters on performance and engine out emissions. Experiments were carried out on a large displacement single cylinder direct injection diesel engine equipped with a high-pressure common rail injection system. The commercial STAR-CD code was used for the simulation of the combustion process calibrating the 3 Zones Extended Coherent Flame Model (ECFM3Z). Tests were performed on different nozzle geometries (147, 150 and 154° spray angle nozzle) and engine parameters such as injection pressure and timing. The main results of the investigation may be summarized as follows:

- the spray angle within the combustion chamber plays a major role in the air-fuel mixing distribution, controlling performance and NOx-smoke trade off,
- the investigation on the injection pressure has highlighted a positive impact on the thermal efficiency, considering the beneficial effect of higher pressures on atomization and mixing rate,
- the numerical simulation has pointed out as the nozzle geometry affect the fuel spray penetration and the air-fuel mixture homogeneity within the combustion chamber,
- the 150° nozzle has given faster burning rates and, as consequence, an enhanced combustion efficiency with lower emissions.

#### **Nomenclature**

ATDC after top dead centre; BDC bottom dead centre; BTDC before top dead centre;

CA crank angle;

CAD crank angle degree;
ROHR Rate of Heat Release;
SOI start of injection;
TDC top dead centre.

#### References

- [1] EPA, Final regulatory impact analysis: control of emissions from marine diesel engines EPA420-R-99-026.
- [2] Ishida, M., Chen, Z., An analysis of the added water effect on NO formation in DI diesel engines, SAE paper 941691, 1994.
- [3] Andrews, G. E., The reduction in diesel particulate emissions using emulsified fuels, SAE 880348, 1988.
- [4] Sarvi, A., Kilpinen, P., Zevenhoven, R., *Emissions from large-scale medium-speed diesel engines: Influence of direct water injection and common rail*, Fuel Processing Technology 90, 222-231, doi:10.1016/j.fuproc.2008.09.003, 2009.
- [5] Fang, T., Lin, Y-C., Foong, T. M., Lee, C-F., *Biodiesel combustion in an optical HSDI diesel engine under low load premixed combustion conditions*, Fuel, 88:2154-62, 2009.
- [6] Lapuerta, M., Armas, O., Rodriguez-Fernandez, J., *Effect of biodiesel fuels on diesel engine emissions*, Progress in Energy and Combustion Science 34, 198–223, doi:10.1016/j.pecs.2007.07.001, 2008.
- [7] Minato, A., Tanaka, T., Nishimura, T., *Investigation of premixed lean diesel combustion with ultra-high- pressure injection*, SAE paper 2005-01-0914, 2005.

- [8] Zhang, W., Nishida, K., Gao, J., Experimental study on mixture formation process of flat wall impinging spray injected by micro-hole nozzle under ultra-high injection pressures, SAE paper 2008-01-1601, 2008.
- [9] Tao, F., Bergstand, P., *Effect of ultra-high injection pressure on diesel ignition and flame under high-boost conditions*, SAE paper 2008-01-1603, 2008.
- [10] Heywood, J. B., Internal Combustion Engine Fundamentals, McGraw-Hill, USA1988.